

Hale COLLAGE 2017 Lecture 14

Flare loop observations: imaging and spectroscopy I



Bin Chen (New Jersey Institute of Technology)

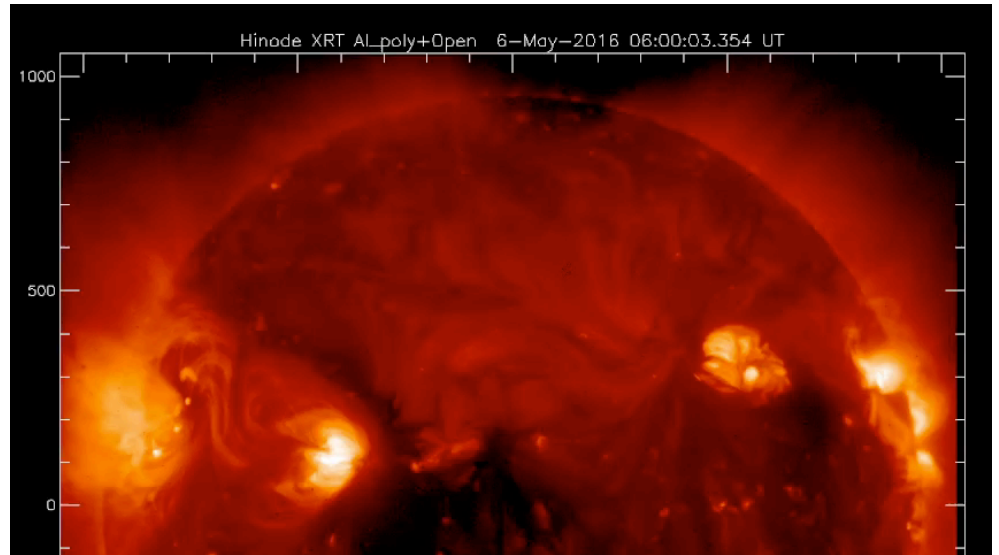
Outline

- Coronal loop observations
 - Hydrostatic loops
 - Hydrodynamic loops
- Suggested reading:
 - Achwanden's book Chapt 3-4

EUV and X-ray loop imaging



SDO/AIA



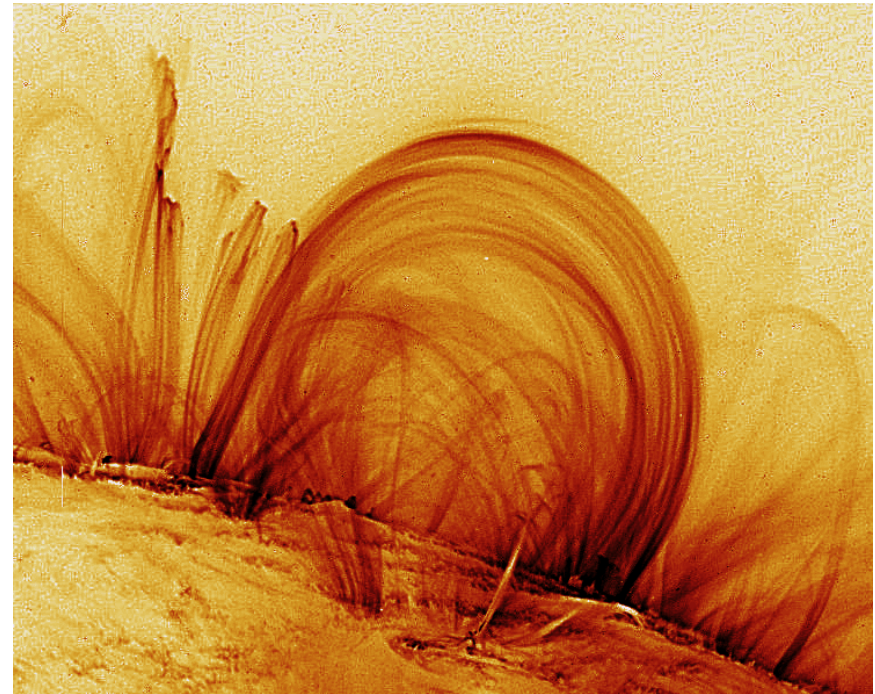
Hinode/XRT

Loop observations

- Loops delineate path of magnetic fields
- Loops have variable scales in length and thickness
- Loops are everywhere
- But loops are visible in EUV and X-ray only if they
 - are dense enough,
 - are thick enough, and
 - have the right temperature for the filter band

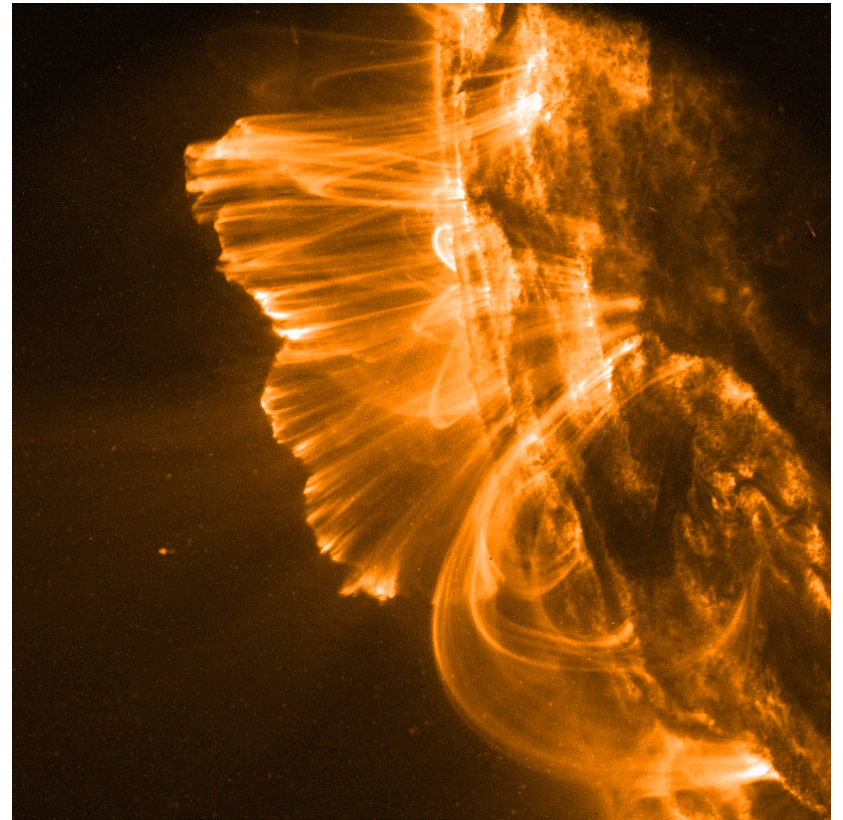
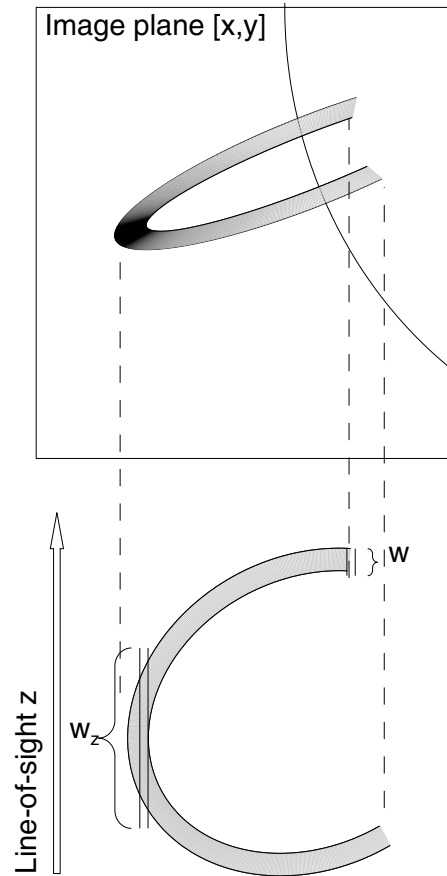
$$B = \int R(T) DEM_c(T) dT$$

$$DEM_c = n_e^2 \frac{d\ell}{dT}$$

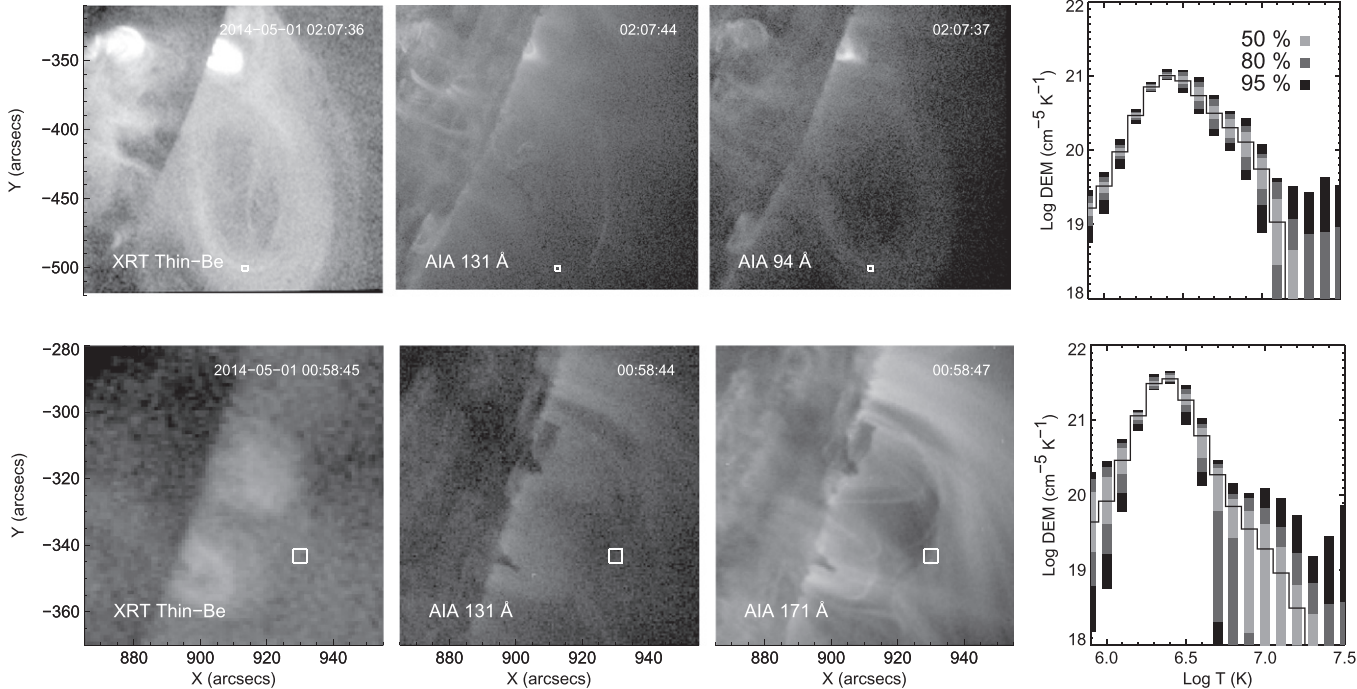


loops observed by TRACE

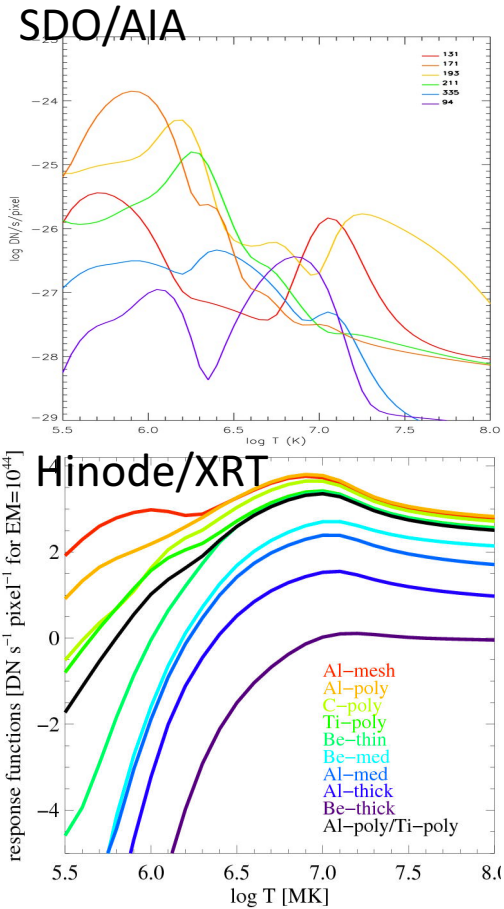
Column depth effect



Effect of instrument response

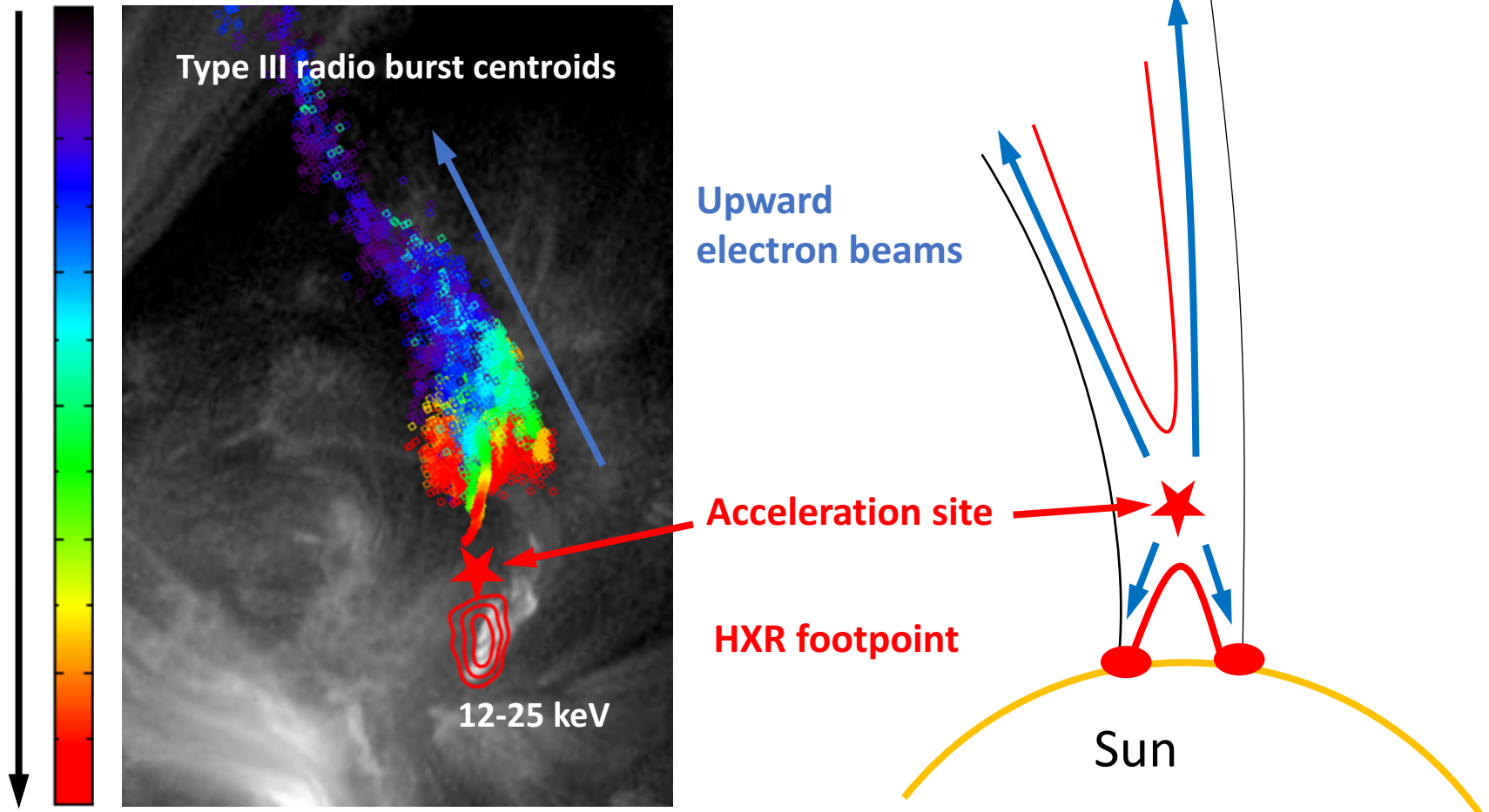


Reeves et al 2015



Electron-beam-conducting loops invisible in EUV

Frequency



Chen et al. 2013

$n_e = \left(\frac{f/2}{8980}\right)^2 \approx 5 \times 10^9 \text{ cm}^{-3}$, $T \sim 1 \text{ MK}$ (from density scale height measurement), but no EUV loop counterparts?

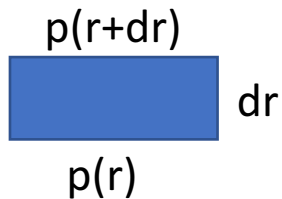
- Probably very thin loops with $d < 100 \text{ km}$

Hydrostatic equilibrium

- Gas pressure balanced only by gravitational force

Grav. force on
single particle

$$F_{grav}(r) = -\frac{d\varepsilon_{grav}(r)}{dr} = -mg_{\odot} \left(\frac{R_{\odot}^2}{r^2} \right)$$



$$\frac{dp}{dr}(r) = \frac{dp_{grav}(r)}{dr} = F_{grav}(r)n(r) = -mn(r)g_{\odot} \left(\frac{R_{\odot}^2}{r^2} \right)$$

$$\rho = mn = m_e n_e + m_i n_i \approx \mu m_H n_e \quad \mu \approx 1.27$$

$$\frac{dp}{dr}(r) = -\mu m_H n_e(r) g_{\odot} \left(\frac{R_{\odot}^2}{r^2} \right) \quad p(r) = 2n_e(r) k_B T_e(r)$$

$$\frac{dp}{dr}(r) = -p(r) \frac{\mu m_H g_{\odot}}{2k_B T_e(r)} \left(\frac{R_{\odot}^2}{r^2} \right)$$

Pressure scale height

$$\frac{dp}{dh}(h) = -p(h) \frac{\mu m_H g_\odot}{2k_B T_e(h)} \left(1 + \frac{h}{R_\odot}\right)^{-2} \quad \text{with} \quad h = r - R_\odot$$

Assuming isothermal plasma: $T_e(h) = T_e$

$$\frac{dp}{p} = -dh \frac{\mu m_H g_\odot}{2k_B T_e} \left(1 + \frac{h}{R_\odot}\right)^{-2} = -\frac{dh}{\lambda_p(T_e)} \left(1 + \frac{h}{R_\odot}\right)^{-2}$$

$$p(h) = p_0 \exp \left[-\frac{(h - h_0)}{\lambda_p(T_e) \left(1 + \frac{h}{R_\odot}\right)} \right] \quad \text{For } h \ll R_\odot$$

Where **pressure scale height**: $\lambda_p(T_e) = \frac{2k_B T_e}{\mu m_H g_\odot} \approx 4.7 \times 10^9 \left(\frac{T_e}{1 \text{ MK}} \right)$

Some remarks

$$p(h) = p_0 \exp \left[-\frac{(h - h_0)}{\lambda_p(T_e) \left(1 + \frac{h}{R_\odot}\right)} \right] \quad \text{For } h \ll R_\odot$$

- $p \sim \text{const.}$ for small variations of h or large T
- Close to surface p decrease exponentially with height
 - For $T = 1$ MK the exponential approx. underestimates the pressure by $\sim 23\%$ at $h=100$ Mm.
- For isothermal case, same height variation for plasma density: $p \propto \rho$

OK, how about B fields?

- A magnetic field \mathbf{B} exerts Lorentz force $\mathbf{j} \times \mathbf{B}$, where \mathbf{j} is the current density
- The force balance now is

$$\nabla p = \rho \mathbf{g} + \mathbf{j} \times \mathbf{B}$$

- Does the equilibrium solution differ from the hydrostatic one?

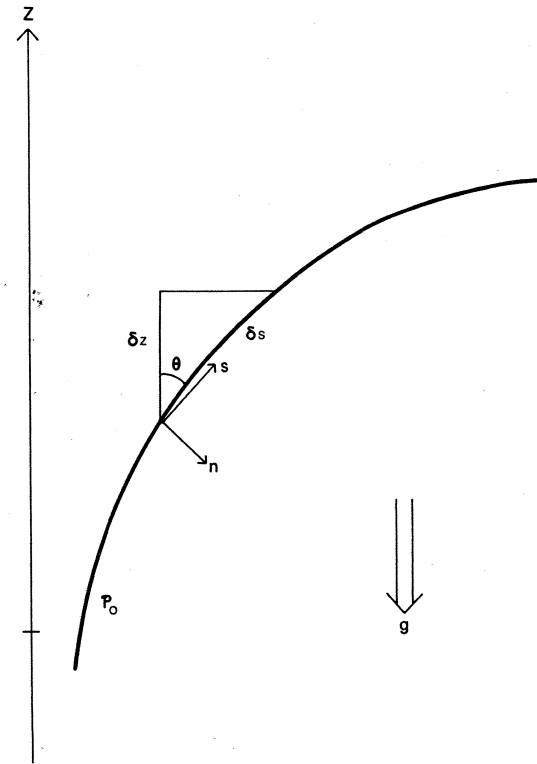
Hydrostatic equilibrium with B fields

- Force balance: $\nabla p = \rho \mathbf{g} + \mathbf{j} \times \mathbf{B}$
- Maxwell's equation: $\nabla \times \mathbf{B} = \frac{1}{c} \frac{\partial \mathbf{E}}{\partial t} + 4\pi \mathbf{j}$
- In nonrelativistic limit, we can neglect the $\frac{1}{c} \frac{\partial \mathbf{E}}{\partial t}$ term, since

$$\frac{1}{c} \frac{\partial \mathbf{E}}{\partial t} \approx \frac{1}{c} \frac{E_0}{t_0} \approx \left(\frac{v_0}{c}\right) \frac{E_0}{l_0} \ll \frac{B_0}{l_0} \approx (\nabla \times \mathbf{B})$$
- So we have $\mathbf{j} = \nabla \times \mathbf{B} / 4\pi$ (Ampere's Law)
- Scalar product by \mathbf{B} to both sides:

$$\mathbf{B} \cdot \nabla p - \rho \mathbf{B} \cdot \mathbf{g} = \mathbf{B} \cdot [(\nabla \times \mathbf{B}) \times \mathbf{B}] / 4\pi$$

Lorentz force. What is its direction?



A note on the Lorentz force

$$\mathbf{j} \times \mathbf{B} = \frac{(\nabla \times \mathbf{B}) \times \mathbf{B}}{4\pi} = -\nabla \left(\frac{B^2}{8\pi} \right) + \frac{1}{4\pi} (\mathbf{B} \cdot \nabla) \mathbf{B}$$

Magnetic pressure

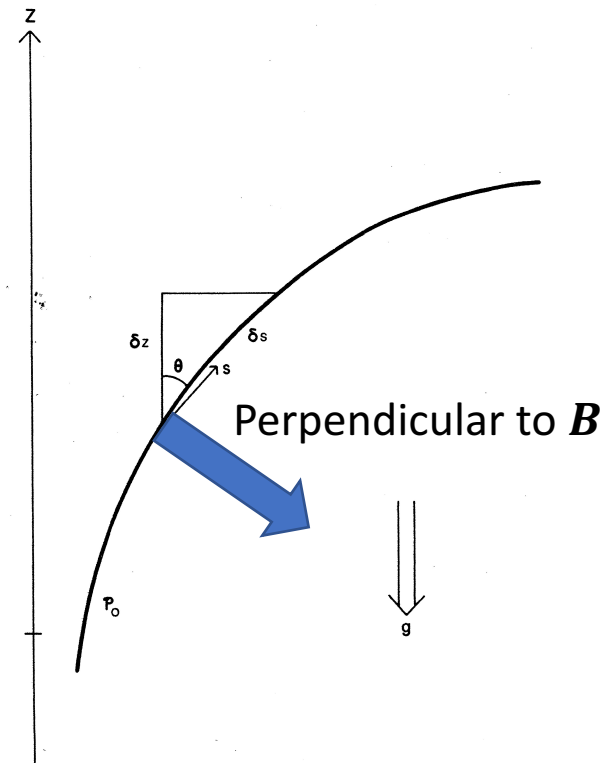
Second term can be further decomposed into two terms:

$$\frac{1}{4\pi} (\mathbf{B} \cdot \nabla) \mathbf{B} = \frac{B}{4\pi} (\hat{\mathbf{b}} \cdot \nabla) B \hat{\mathbf{b}} = \hat{\mathbf{b}} \hat{\mathbf{b}} \cdot \nabla \left(\frac{B^2}{8\pi} \right) + \frac{B^2}{4\pi} (\hat{\mathbf{b}} \cdot \nabla) \hat{\mathbf{b}}$$

Magnetic pressure gradient parallel to \mathbf{B} , which cancels the component in the first term

Magnetic tension

$$= -\frac{B^2 \hat{\mathbf{r}}}{4\pi r_c}$$



$$\mathbf{j} \times \mathbf{B} = \frac{(\nabla \times \mathbf{B}) \times \mathbf{B}}{4\pi} = -\nabla_{\perp} \left(\frac{B^2}{8\pi} \right) - \frac{B^2 \hat{\mathbf{r}}}{4\pi r_c}$$

For a dipole field, the two terms cancel each other

Hydrostatic equilibrium with B fields

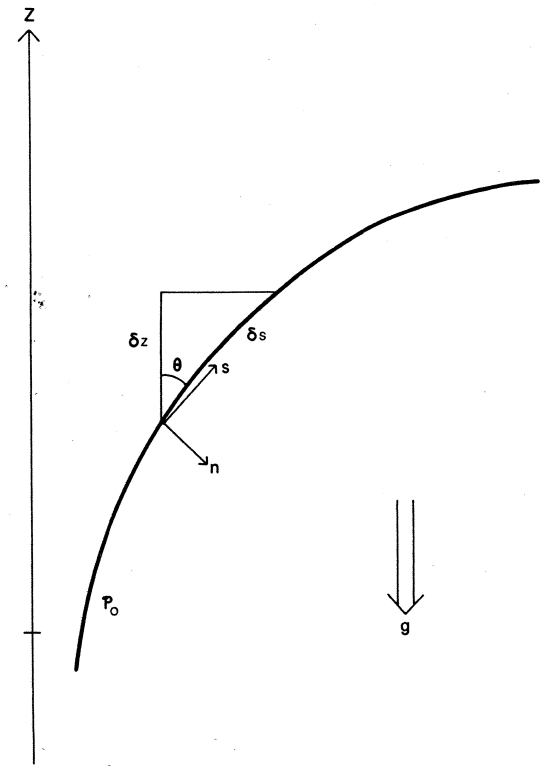
$$\mathbf{B} \cdot \nabla p - \rho \mathbf{B} \cdot \mathbf{g} = \mathbf{B} \cdot \frac{(\nabla \times \mathbf{B}) \times \mathbf{B}}{4\pi} = 0$$

$$-B \frac{dp}{ds} - \rho B g \cos \theta = 0$$

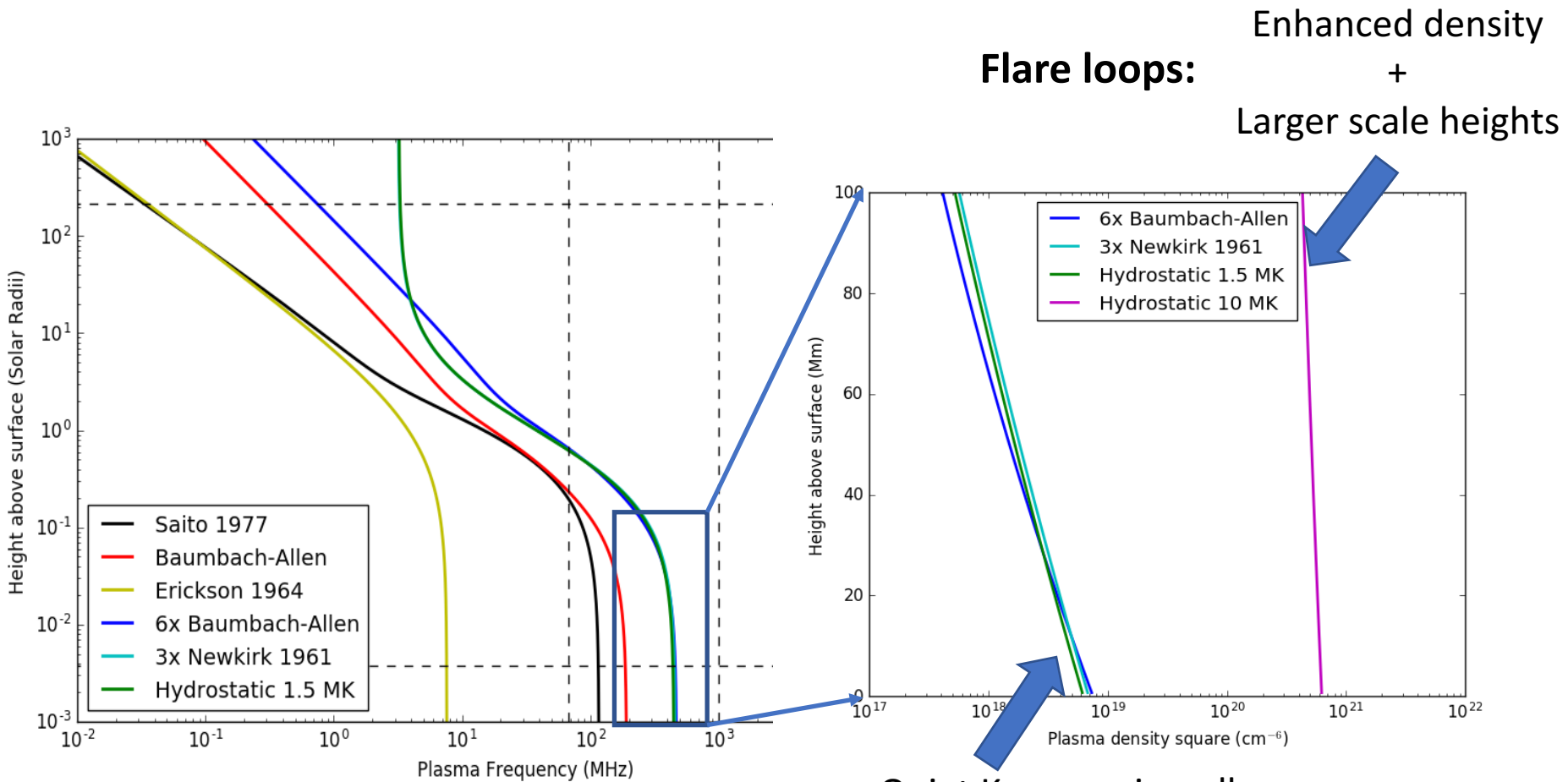
↓ $ds = dz / \cos \theta$

$$\frac{dp}{dz} + \rho g = 0$$

- Same equation as the hydrostatic case
 - Same vertical dependence of density and pressure
 - However, each loop can have its own T and λ , so they can behave differently
 - Each loop acts like a mini solar atmosphere!



Hydrostatic isothermal density model

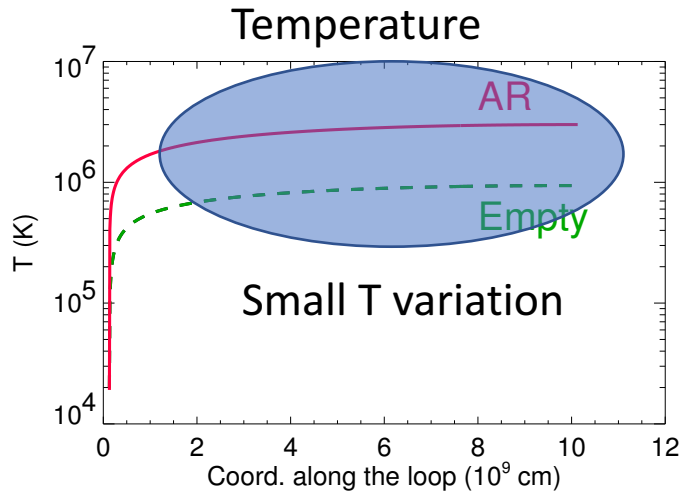


PS #2 question #2

Flare loops: Enhanced density + Larger scale heights

Quiet K corona is well approximated by an exponential density model

More realistic hydrostatic loops

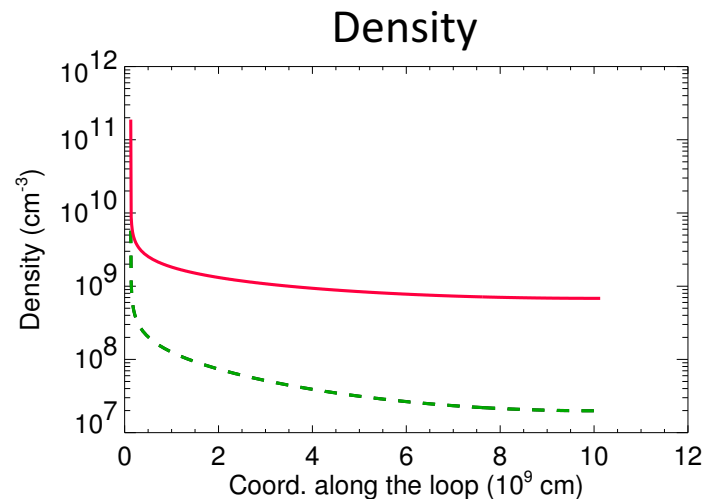
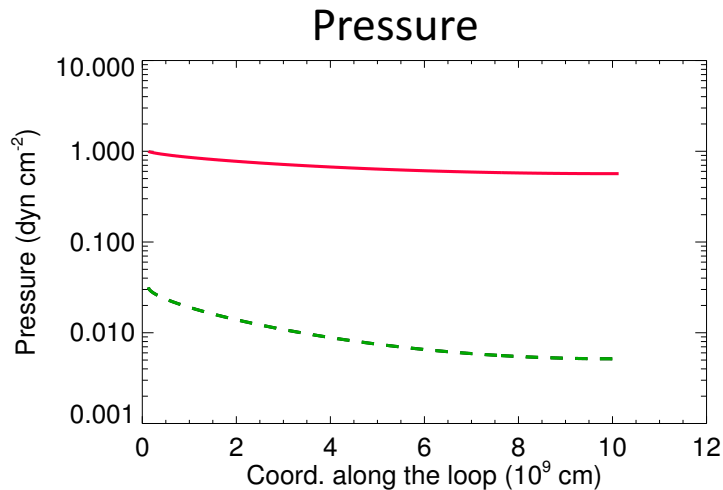


Need to account for temperature change from chromosphere to transition region to corona.

$$\frac{dp}{ds} - \frac{dp_{grav}}{dr} \left(\frac{dr}{ds} \right) = 0,$$

$$E_H(s) - E_R(s) - \frac{1}{A(s)} \frac{d}{ds} A(s) F_C(s) = 0$$

Heating Radiation Conduction



Simulation by Serio et al. 1981

Are AR loops in hydrostatic equilibrium?

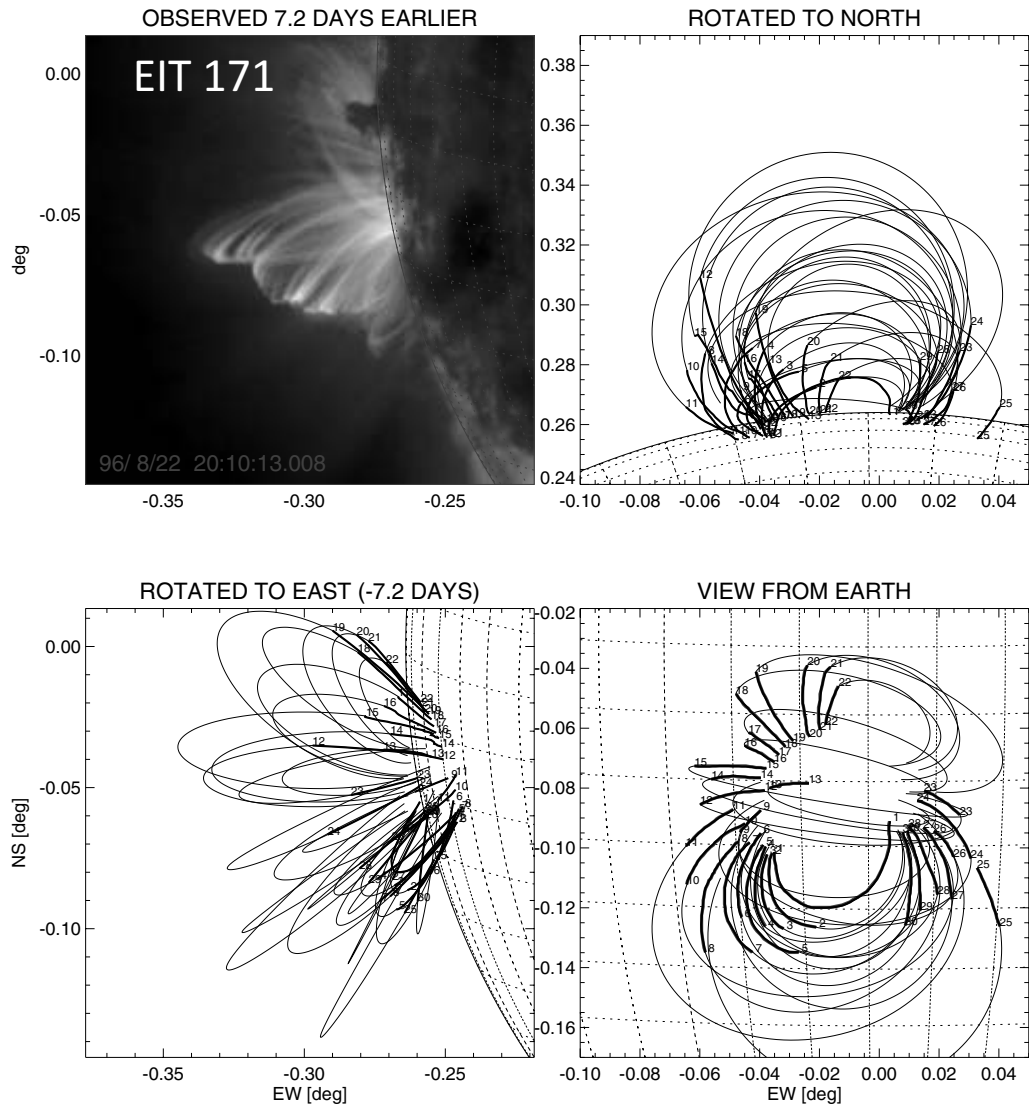
- TRACE/AIA 171 images are sensitive to ~ 1 MK plasma
- Hydrostatic equilibrium: $n(h) = n_0 \exp\left(-\frac{h-h_0}{\lambda_n}\right)$ with $\lambda_n \sim 47$ Mm
- The image intensity is proportional to n^2 , so

$$I(h) \approx I_0 \exp\left[-\frac{2(h-h_0)}{\lambda_n}\right]$$

intensity scale-height is $\lambda_I \sim \lambda_{EM} \sim 24$ Mm

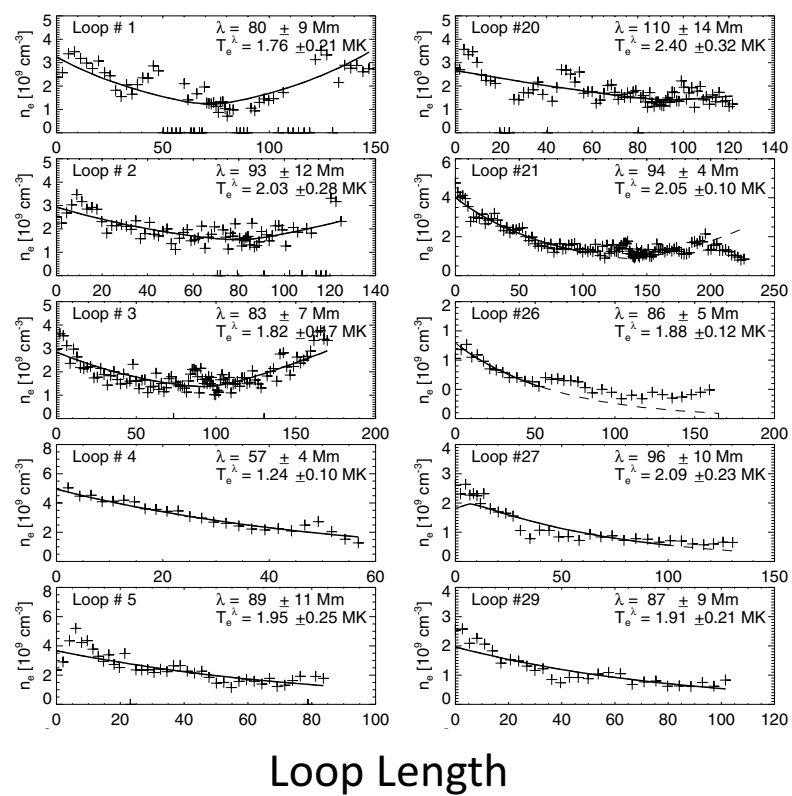
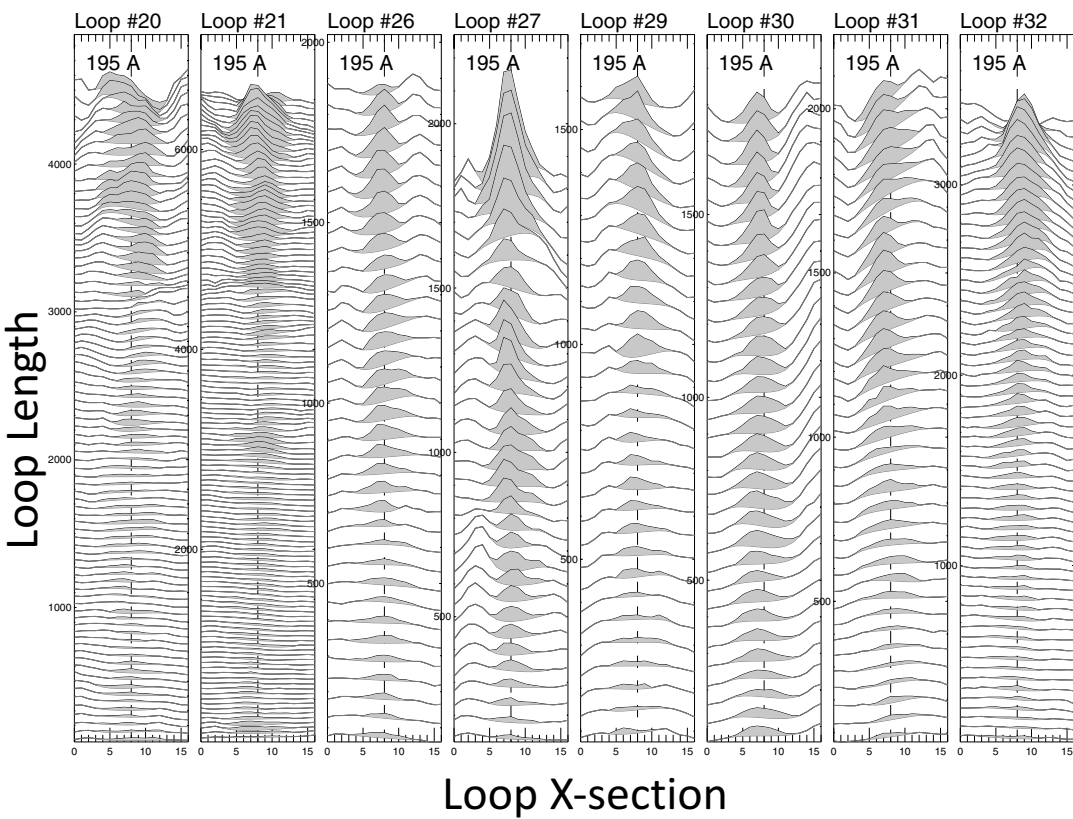
- Intensity decreases by almost 40% every 24 Mm
- Is this what we usually observe for AR loops?

Observation of an “old” AR loop system



Aschwanden et al. 1999

Hydrostatic AR loops



Scaling laws for hydrostatic loops

Simplification/assumptions:

- Hydrostatic equilibrium
- Symmetry w.r.t. apex
- Length shorter than λ_p : nearly constant pressure p
- Heat deposited uniformly along loop ($h/Q/E=\text{const.}$)

$$T_{0,6} = 1.4 (pL_9)^{1/3}$$

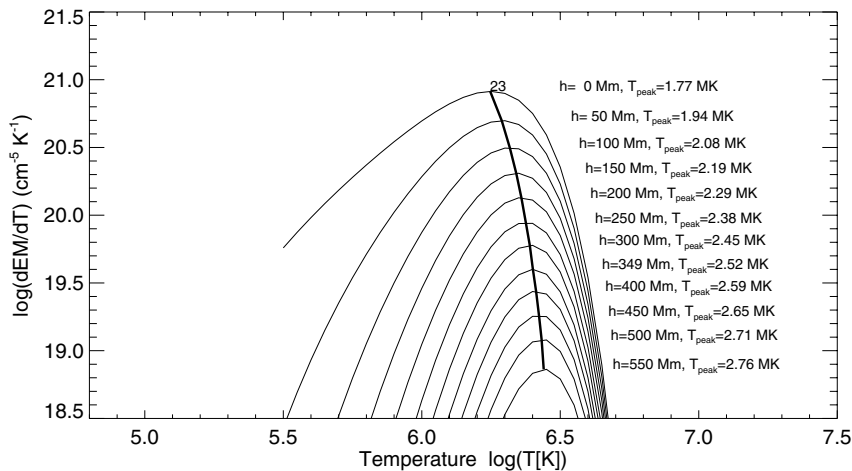
$$H_{-3} = 3p^{7/6} L_9^{-5/6},$$

- Known as “RTV” scaling laws (after Rosner, Tucker, and Vaiana)
- Matches observations from Skylab X-ray data within a factor of 2
- Hydrostatic equilibrium describes some coronal loops fairly well

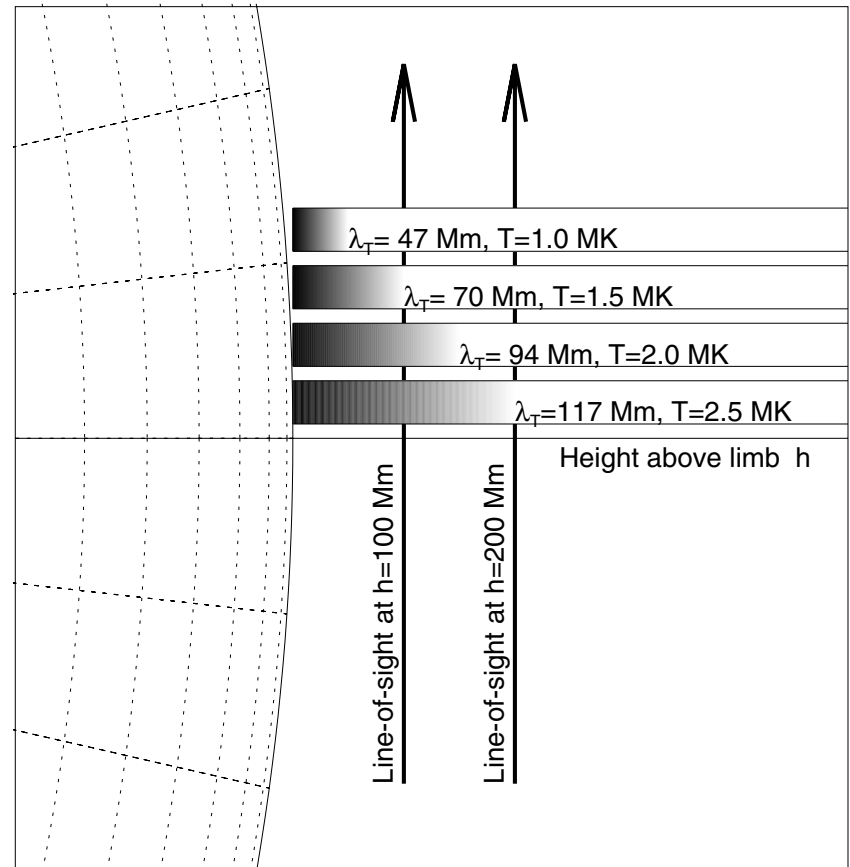
Rosner et al 1978

Multi-thermal corona and hydrostatic weighting bias

- Measured EUV/X-ray intensity have contribution from multiple loops along LOS
- Relative contribution to intensity from hotter loops is greater at increasing heights

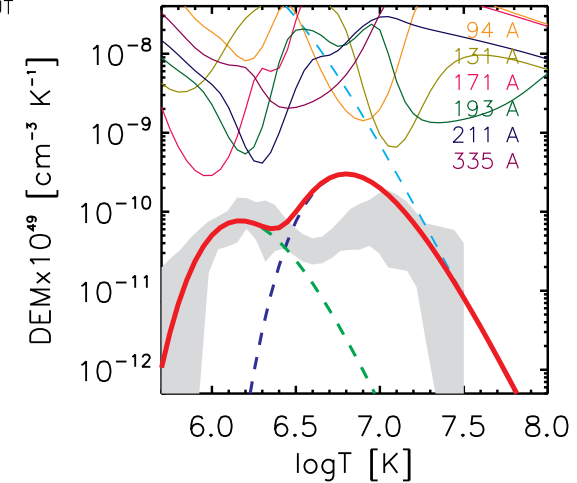
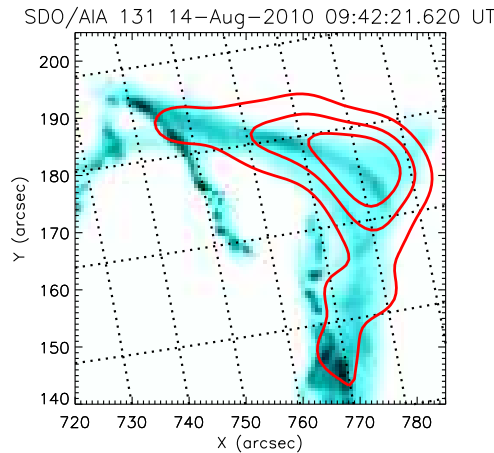
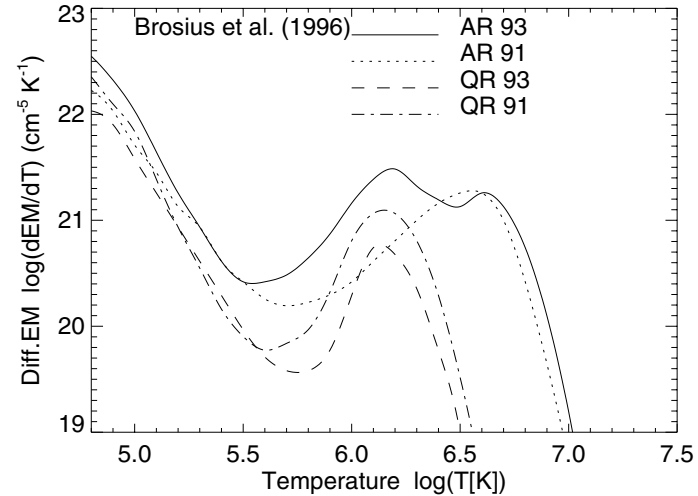
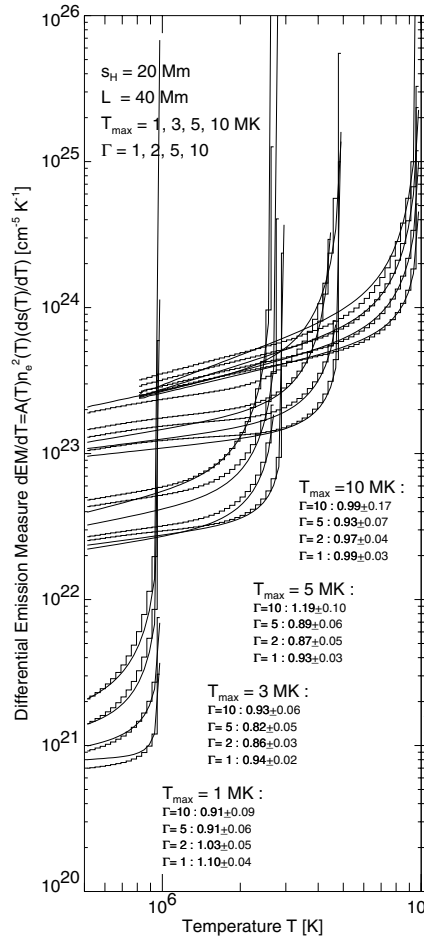


Aschwanden & Acton 2001



Aschwanden & Nita 2000

Contribution to DEM from hot loops

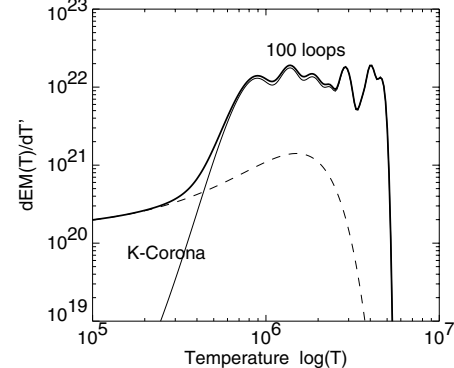
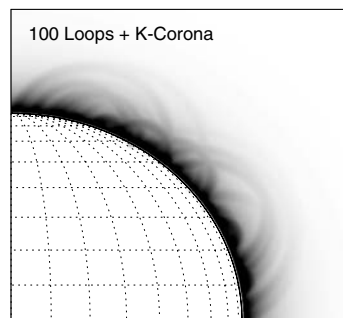
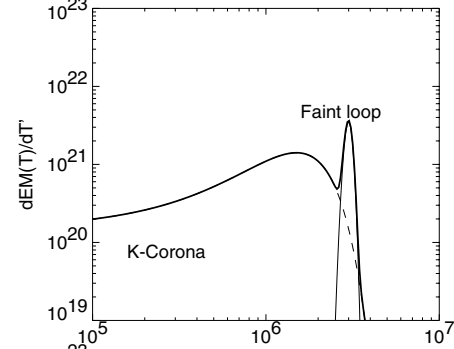
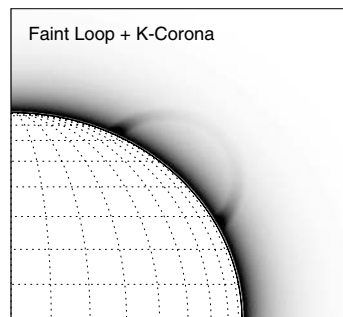
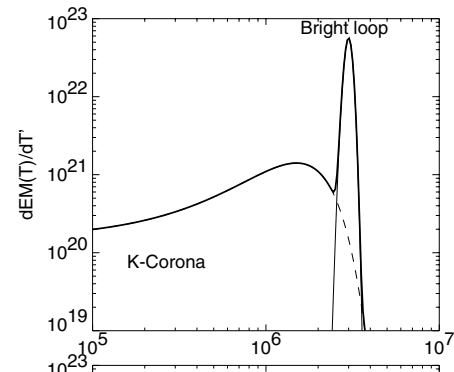
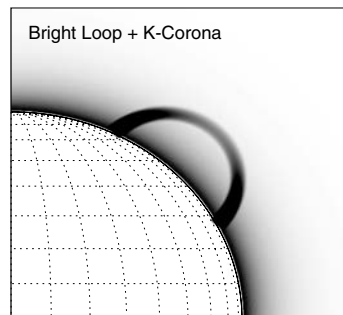
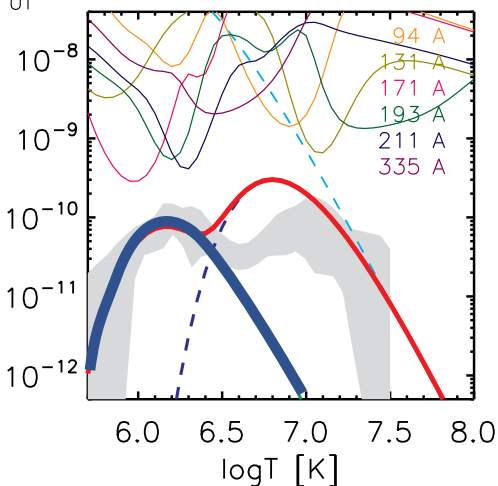
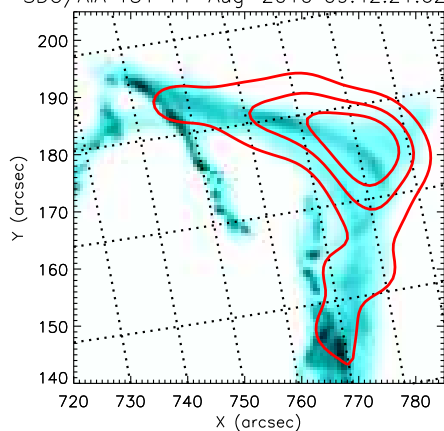


Contribution to DEM from hot loops is orders of magnitude higher than cool loops!

Battaglia et al 2015

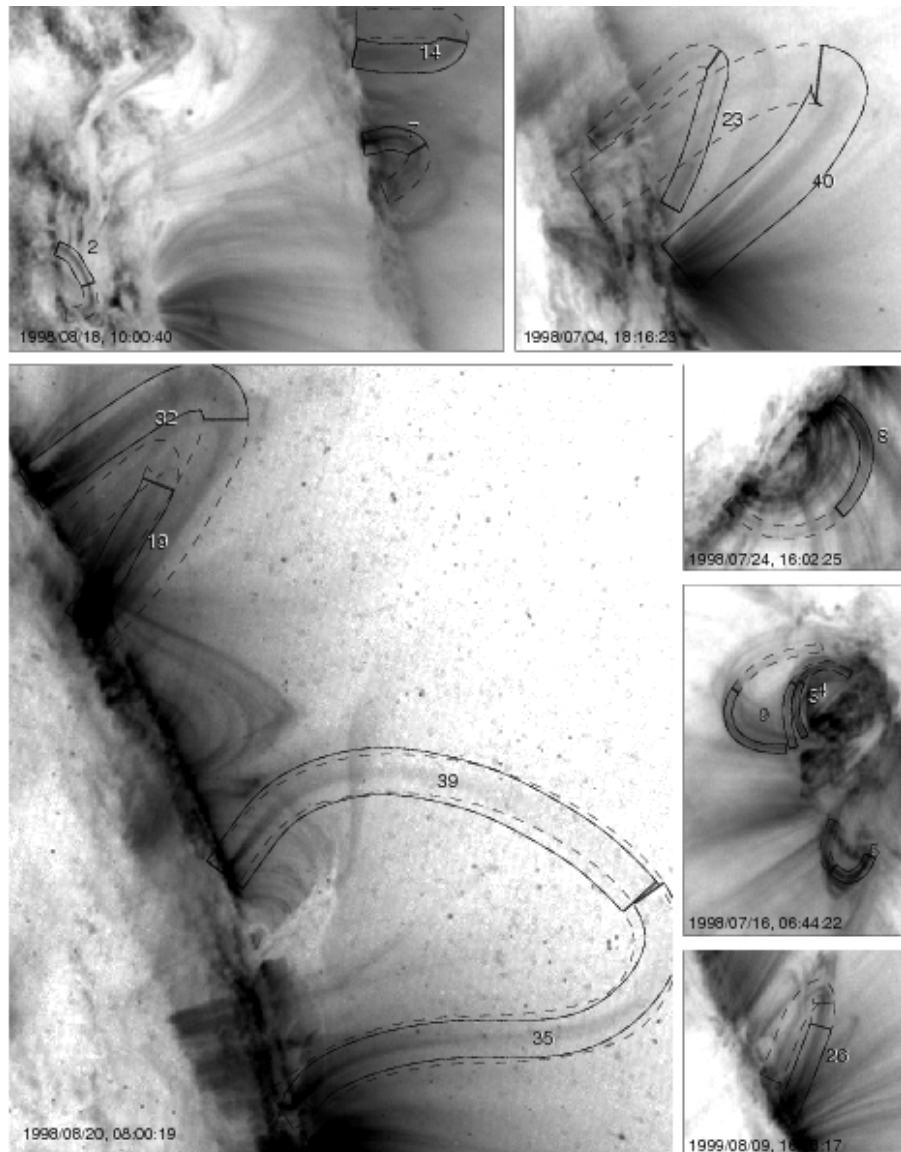
DEM with broad T distribution, why?

SDO/AIA 131 14-Aug-2010 09:42:21.620 UT



- Active regions usually have many loops with different sizes, temperature, and density
- Any line of sight would inevitably encounter many of these loops + background K-corona
- A broad DEM distribution peaking at 1-3 MK is common in DEM inversion results

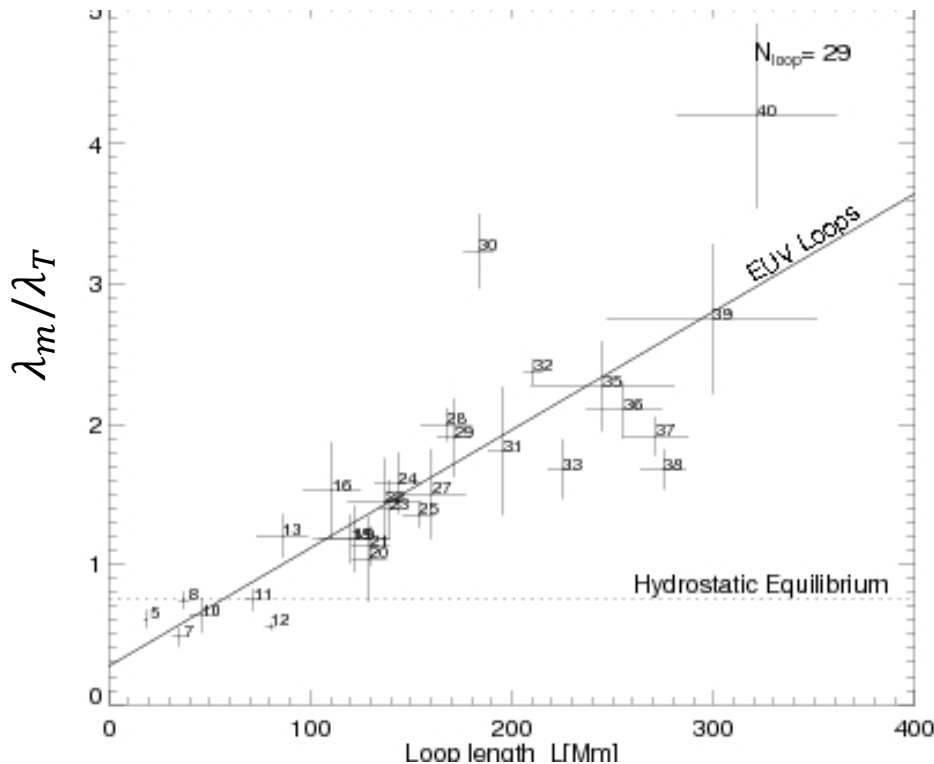
AR loops not in hydrostatic equilibrium



- 40 loops analyzed by Aschwanden et al. 2000, measure intensity vs. loop length
- Infer a measured scale-height (λ_m)
- Loops selected if intensity contrast is significant along their whole length
- But, suppose a long loop is in hydrostatic equilibrium, intensity decreases substantially from bottom to top
- Long loops in hydrostatic equilibrium cannot be detected with this selection criterion

AR loops not in hydrostatic equilibrium

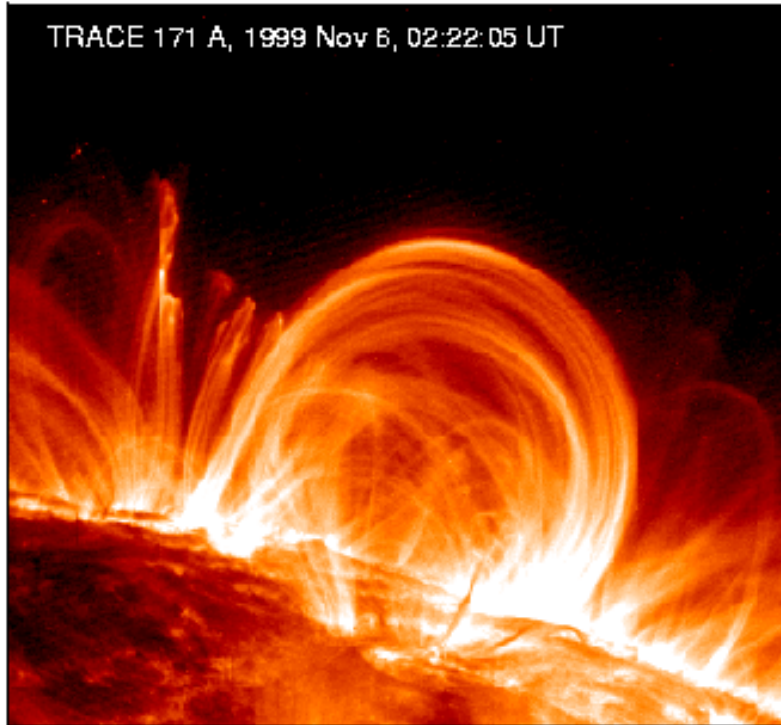
- Results: only a few loops have $\lambda_m \sim \lambda_T$, all other loops are not in hydrostatic equilibrium



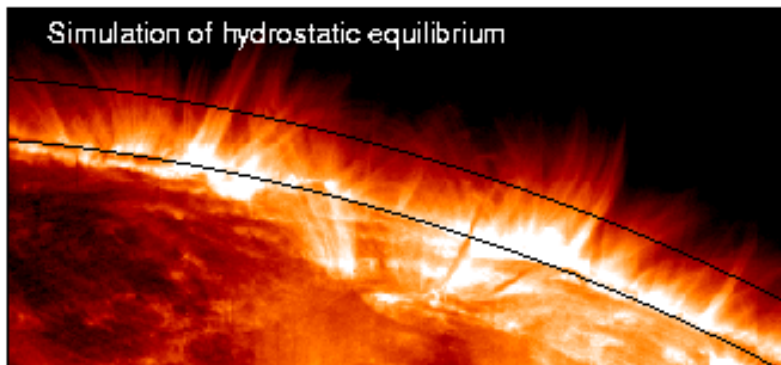
No long loops in hydrostatic equilibrium found (as expected)

In fact, many loops are not in hydrostatic equilibrium

Are AR loops in hydrostatic equilibrium?

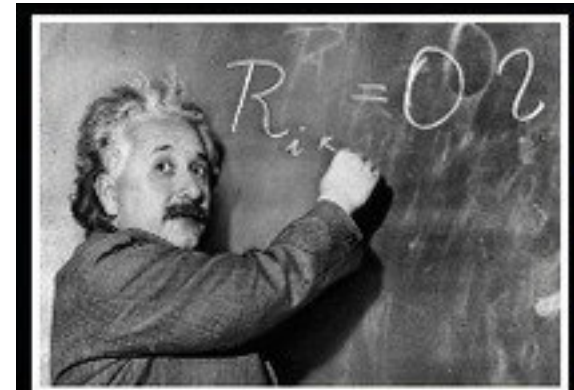


How active region loops look like in TRACE 171

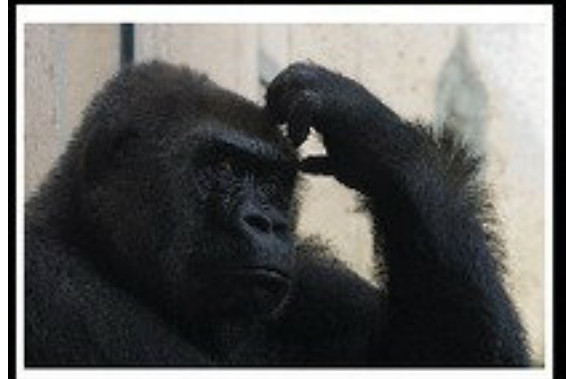


How they would look like if in hydrostatic equilibrium

Physicist



WHAT SOCIETY THINKS I DO



WHAT I ACTUALLY DO

What's wrong?

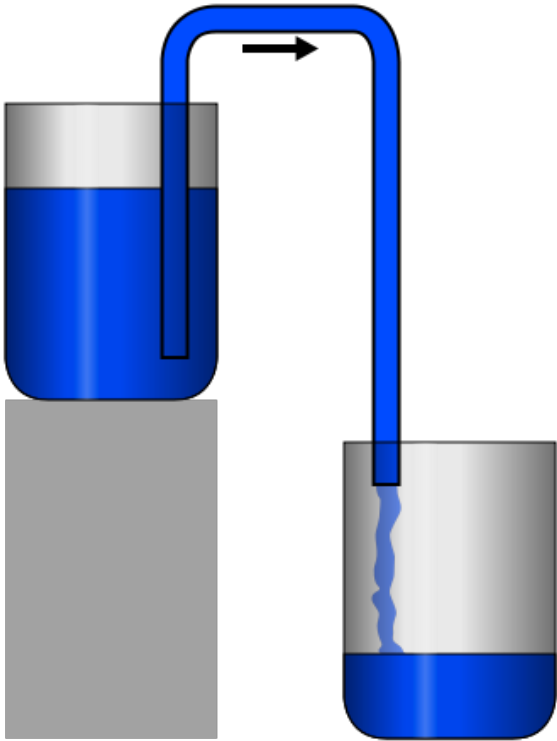
- Maybe our assumption of hydrostatic equilibrium is not valid in the first place?

$$\rho \frac{Dv}{Dt} \neq 0$$

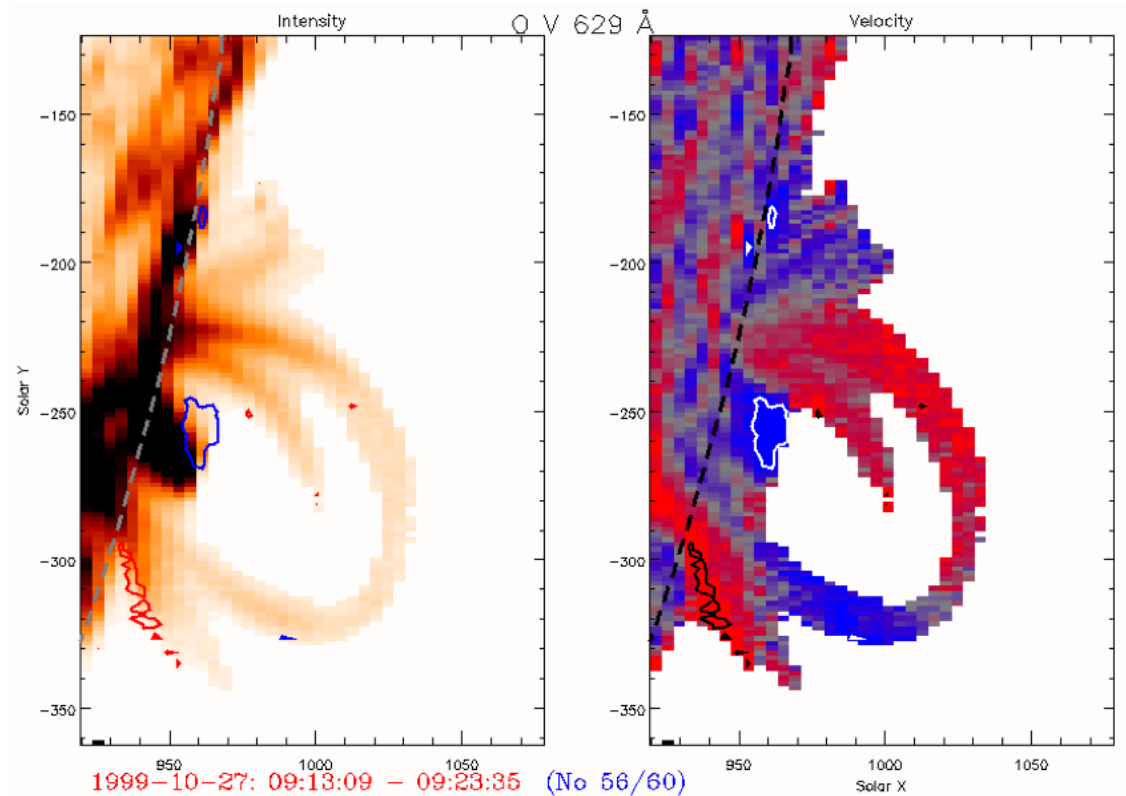
- OK, let's consider hydrodynamic loops, starting from those with steady flows:

$$\rho \frac{Dv}{Dt} = \rho \cancel{\frac{\partial v}{\partial t}} + \rho v \frac{\partial v}{\partial s}$$

Dynamic loops: steady flows



“Siphon” flow



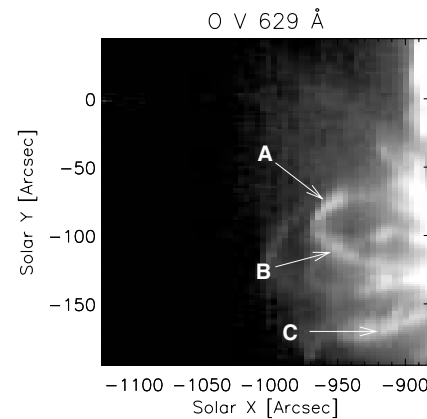
Observed by SOHO/CDS

However, impossible to distinguish in imaging observations!

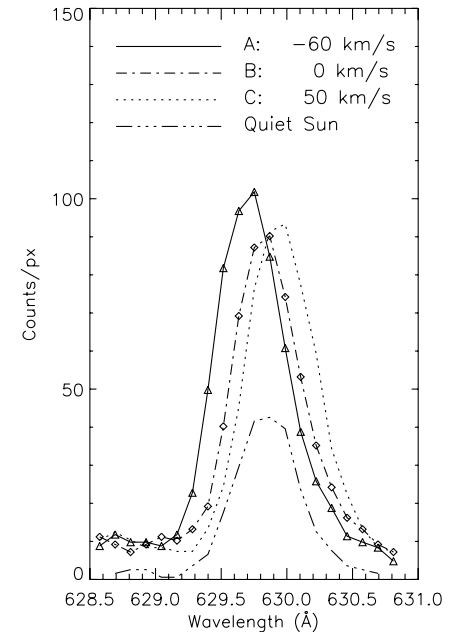
Observations of flows in AR loops

Methods:

- Spectroscopy: Doppler shifts of spectral lines
- Imaging: Inhomogeneities in flowing plasma



Brekke et al 1997



Active region loops:

Brekke et al. (1997a)	SoHO/CDS	Mg IX, 368 Å	1.0 MK	$< 50 \text{ km s}^{-1}$
	SoHO/CDS	Mg X, 624 Å	1.0 MK	$< 50 \text{ km s}^{-1}$
	SoHO/CDS	Si XII, 520 Å	1.9 MK	$\approx 25 \text{ km s}^{-1}$
	SoHO/CDS	Fe XVI, 360 Å	2.7 MK	$\approx 25 \text{ km s}^{-1}$
Winebarger et al. (2001)	TRACE	Fe IX/X, 171 Å	1.0 MK	$5 - 20 \text{ km s}^{-1}$
Winebarger et al. (2002)	SUMER	Ne VIII, 770 Å	0.6 MK	40 km s^{-1}

Steady flows: adiabatic solutions

$$\frac{1}{A} \frac{\partial}{\partial s} (n v A) = 0, \quad \text{Continuity equation}$$

$$m n v \frac{\partial v}{\partial s} = - \frac{\partial p}{\partial s} + \frac{\partial p_{grav}}{\partial r} \left(\frac{\partial r}{\partial s} \right), \quad \text{Momentum equation}$$

$$p \rho^{-\gamma} = \text{const} \quad \text{Adiabatic assumption}$$

Consider constant gravity (near surface) and semi-circular loops:

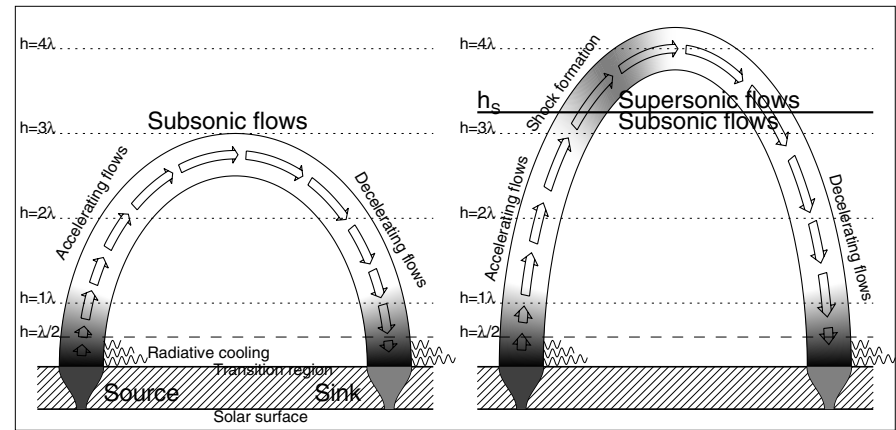
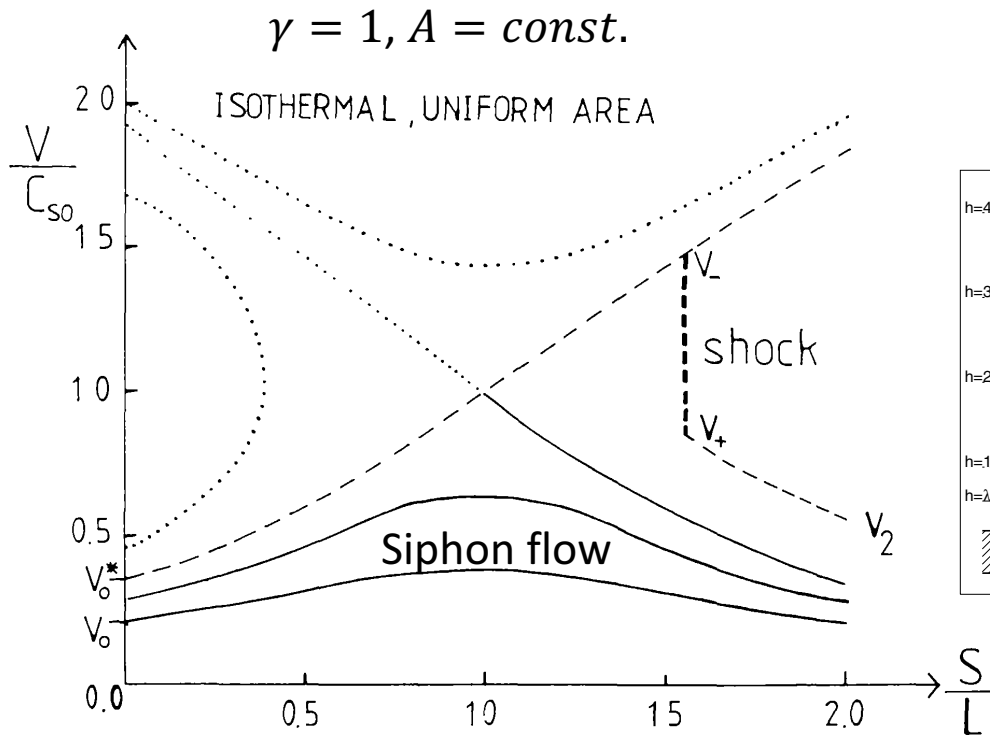
$$\partial p_{grav} / \partial r \approx -m n g_{\odot}$$

$$\partial r / \partial s = \cos(\pi s / 2L)$$

We can derive a differential equation for the flow speed $v(s)$:

$$\left(v - \frac{c_s^2}{v} \right) \frac{\partial v}{\partial s} = -g_{\odot} \cos\left(\frac{\pi s}{2L}\right) + \frac{c_s^2}{A} \frac{\partial A}{\partial s}$$

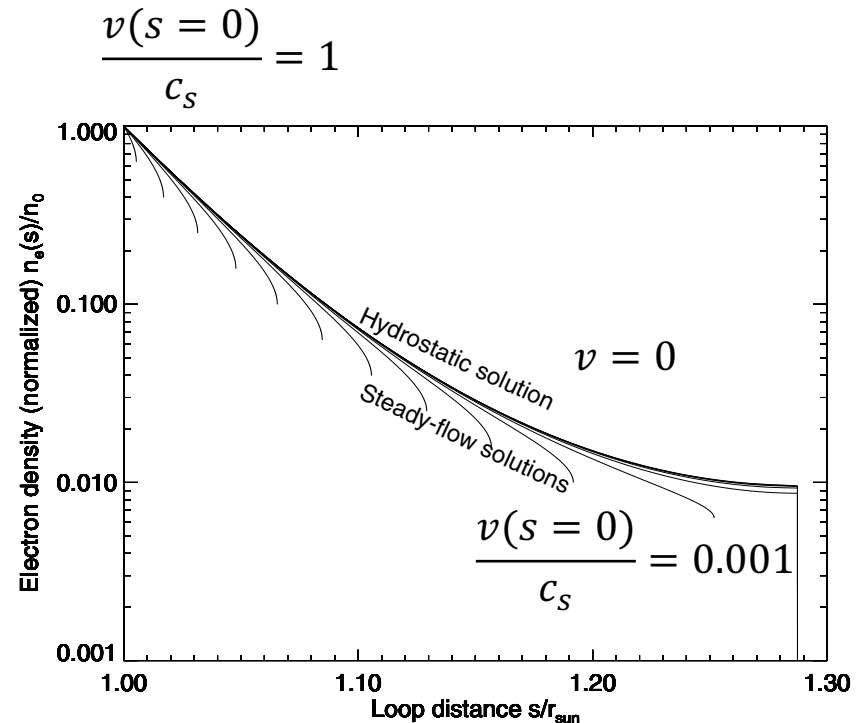
Steady flows: isothermal case



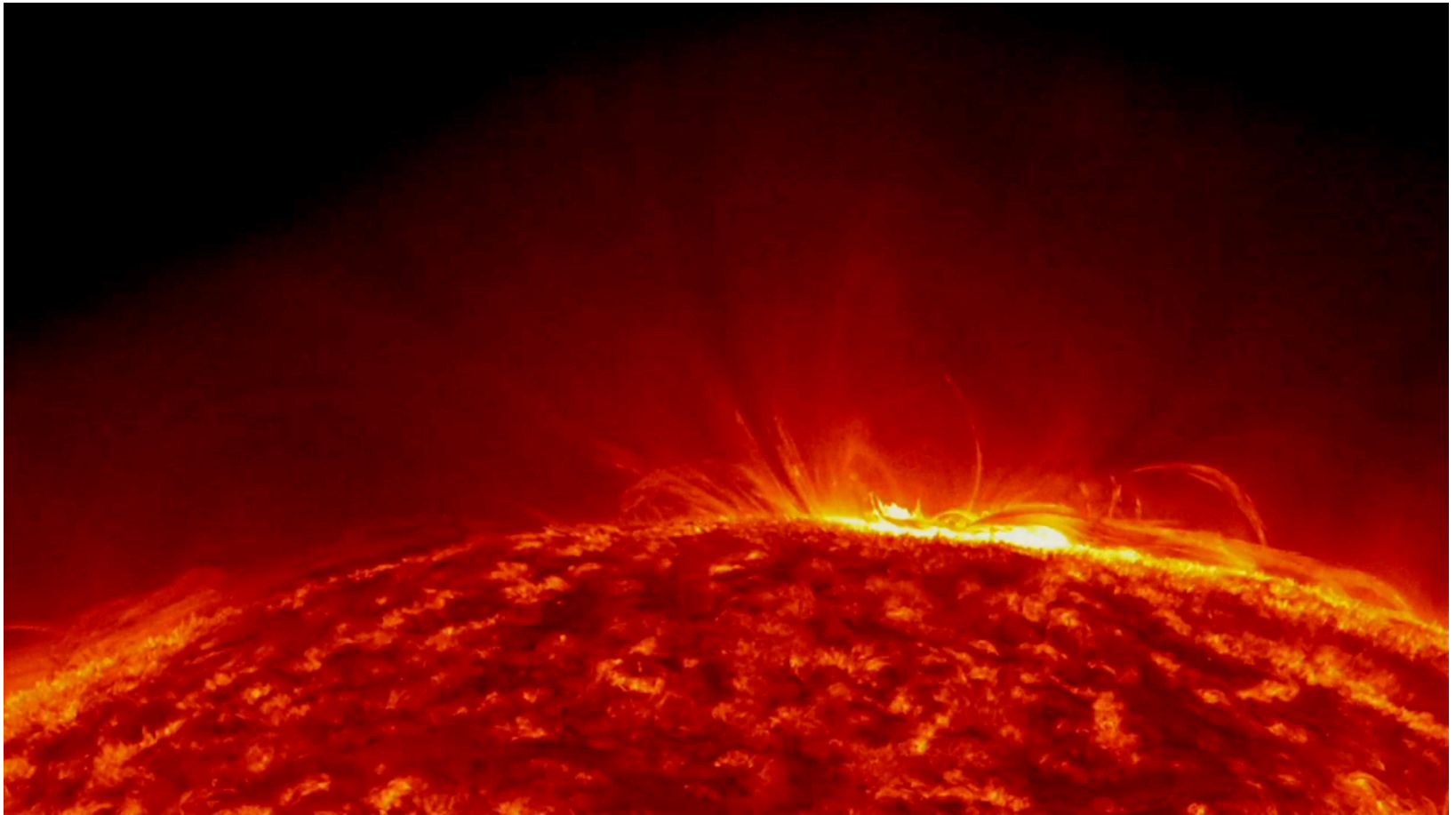
Cargill & Priest 1980

Density profiles for loops with steady flows

- Density profiles for loops with steady flows are not very different from the hydrostatic case up to the sonic point
- So what causes the super-hydrostatic loops?
 - Time-dependent flows
 - Energetics must be taken into account (impulsive and nonuniform heating & cooling)
 - Waves or magnetic field may play a role



Another type of flow: coronal rain



Post-flare coronal rain observed by SDO/AIA 304 on 2012 July 19

Radiative loss instability

Let's ignore thermal conduction loss for now:

$$c_p \rho \frac{\partial T}{\partial t} = E_H - E_R$$

Heating Radiative loss

$E_H = h\rho$ where h is the (constant) heating rate per unit volume

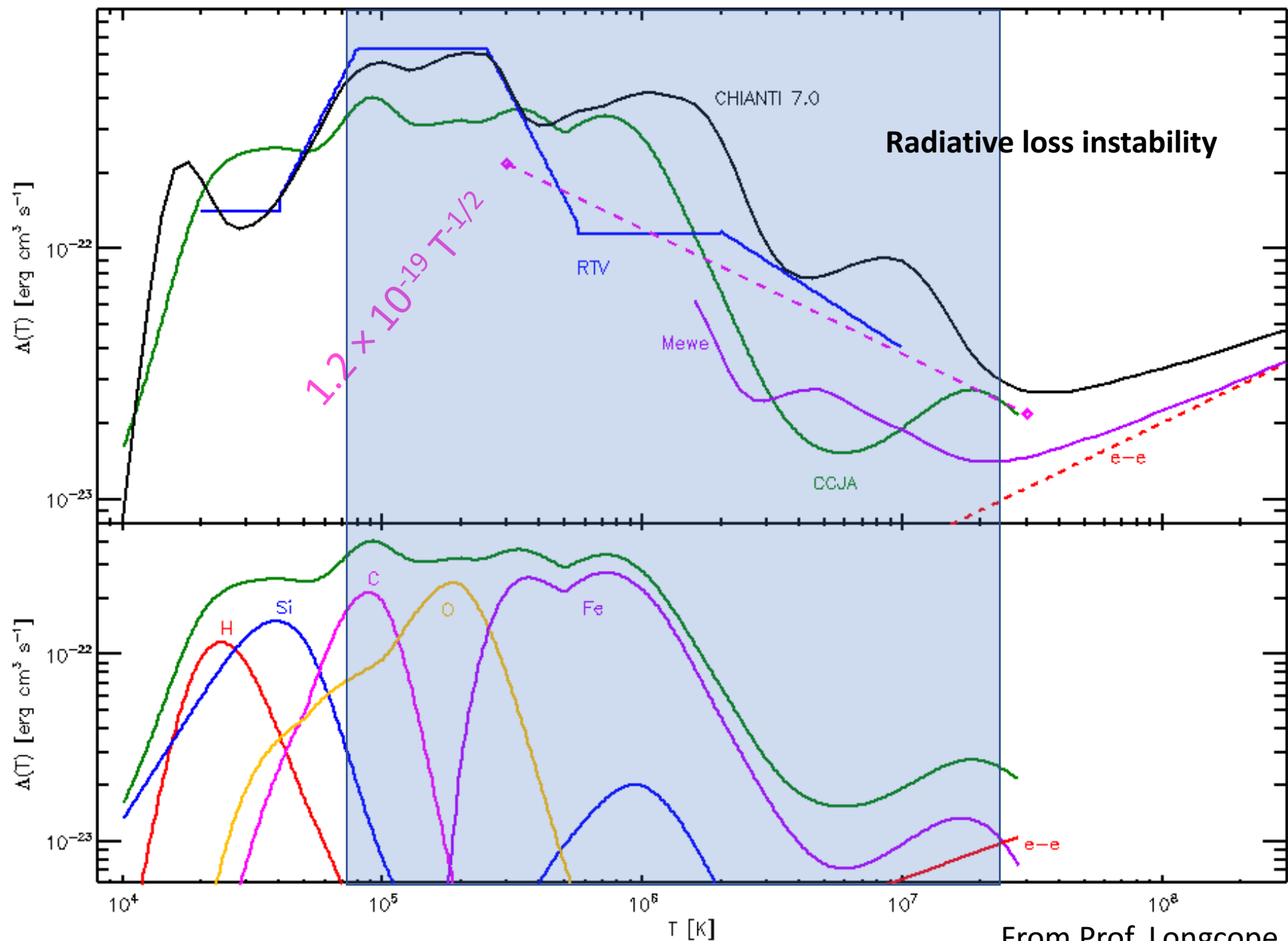
$$E_R = n^2 \Lambda(T) \approx \chi \rho^2 T^\alpha$$

Assume constant pressure and initially thermal equilibrium

$$h - \chi \rho_0 T_0^\alpha (s) = 0, \text{ where } \rho_0 = mp_0/k_B T_0$$

$$c_p \frac{\partial T}{\partial t} = \chi \rho_0 T_0^\alpha \left(1 - \frac{T^{\alpha-1}}{T_0^{\alpha-1}} \right)$$

$\alpha < 1$: once $T < T_0$, $c_p \frac{\partial T}{\partial t} < 0$, cooling continues  **Instability!**



From Prof. Longcope

Coronal rain: catastrophic cooling process

Slow radiative cooling



Lower temperature



$$p = nk_B T$$

Clumping and catastrophic cooling

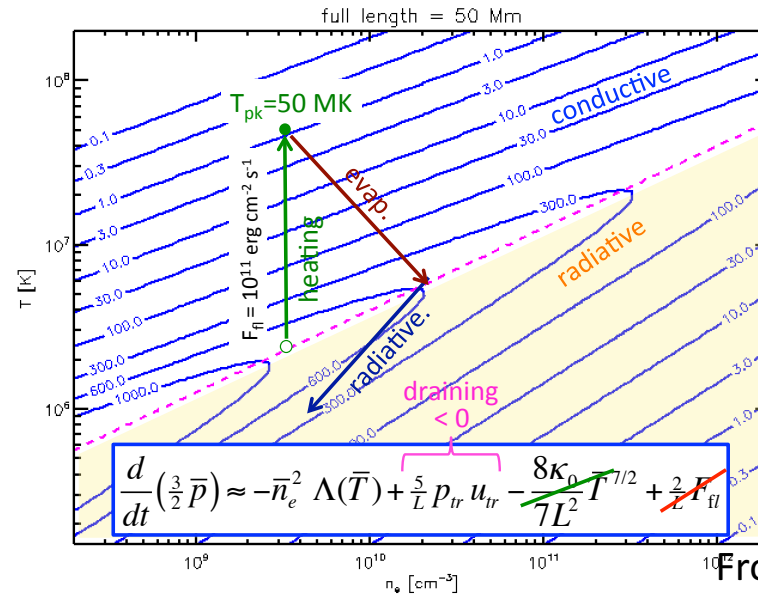


“Condensation”

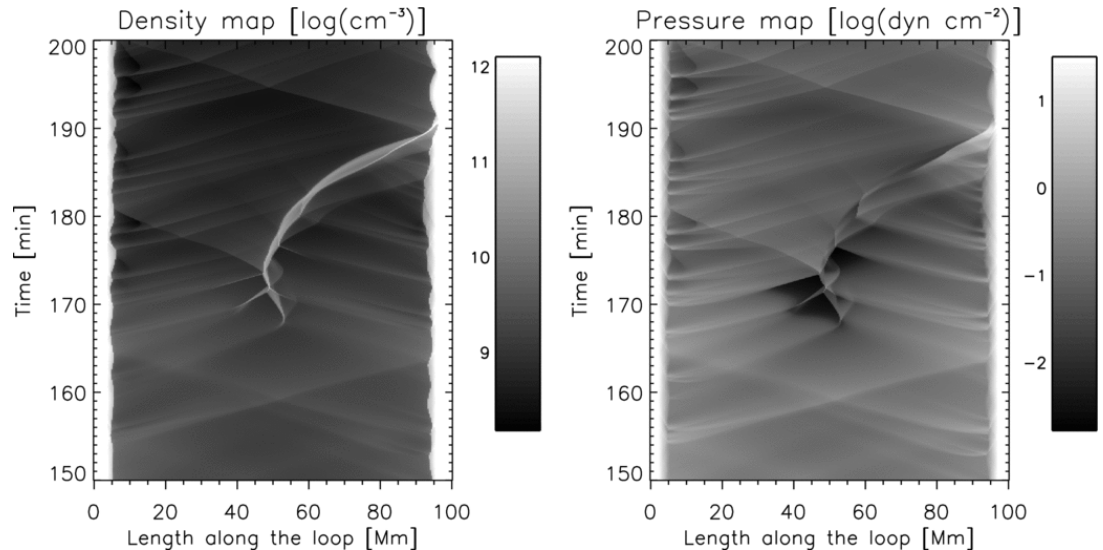


Draining

Antiochos et al. 1999

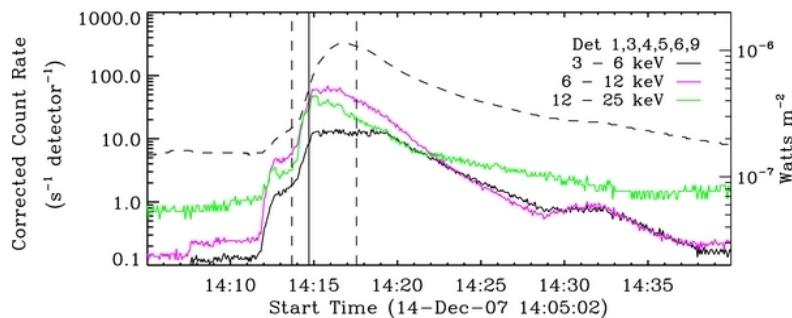
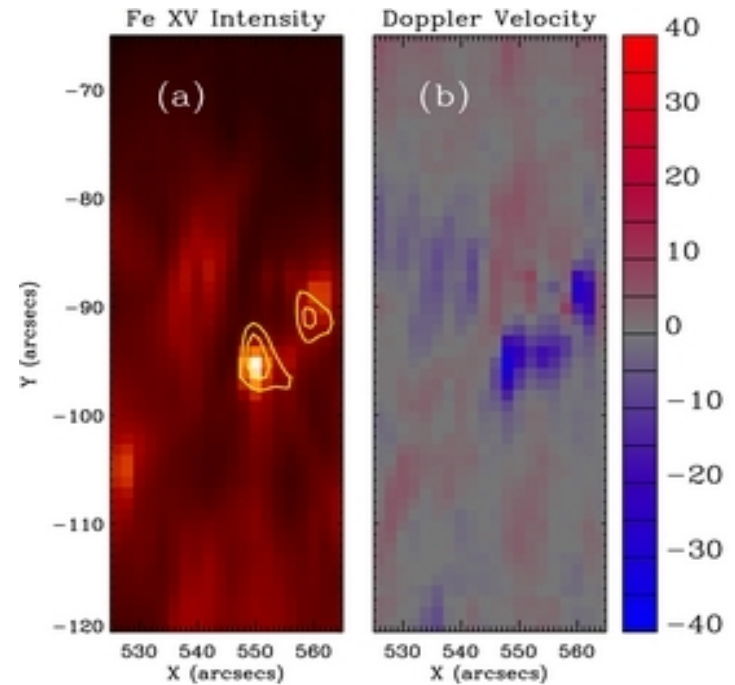
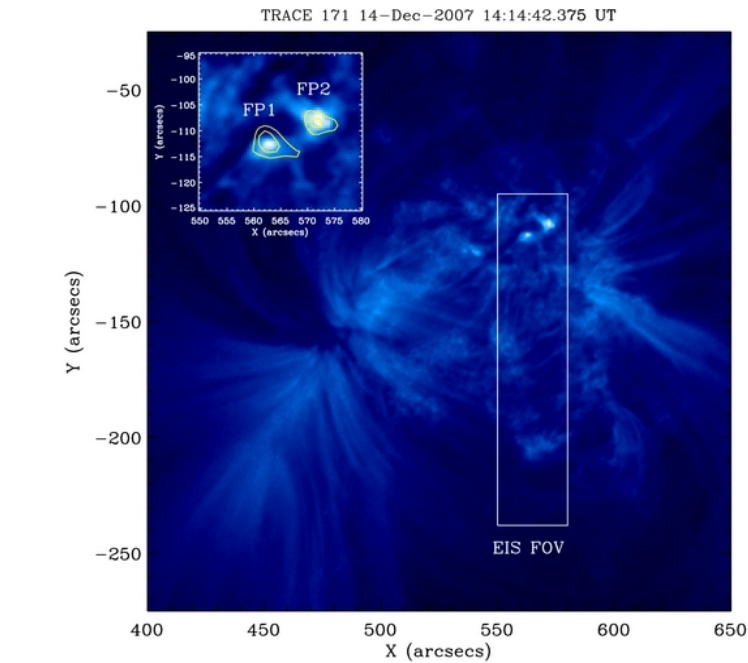


From Prof. Longcope



Antolin et al. 2010

And of course, evaporation flows in flare loops



Hinode/EIS

Milligan 2011

Summary

- Imaging observations of loops are highly weighted by loop density and instrument response
- Hydrostatic approximation for loops works surprisingly well in some cases
- Non-hydrostatic loops are important, esp. in active regions and flares
- Yet simple approximations greatly help us understand the observations!